

Microstructural evolution in H ion induced splitting of freestanding GaN

O. Moutanabbir,^{1,a)} R. Scholz,¹ S. Senz,¹ U. Gösele,¹ M. Chicoine,² F. Schiettekatte,² F. Süßkraut,³ and R. Krause-Rehberg³

¹Max Planck Institute of Microstructure Physics, Weinberg 2, D 06120 Halle, Germany

²Département de Physique, Université de Montréal, Succursale Centre Ville, Montréal, Québec, H3T 1J4, Canada

³Department of Physics, Martin-Luther-University Halle-Wittenberg, Friedemann-Bach-Platz 6, D 06108 Halle, Germany

(Received 24 April 2008; accepted 12 June 2008; published online 25 July 2008)

We investigated the microstructural transformations during hydrogen ion-induced splitting of GaN thin layers. Cross-sectional transmission electron microscopy and positron annihilation spectroscopy data show that the implanted region is decorated with a high density of 1–2 nm bubbles resulting from vacancy clustering during implantation. These nanobubbles persist up to 450 °C. Ion channeling data show a strong dechanneling enhancement in this temperature range tentatively attributed to strain-induced lattice distortion. The dechanneling level decreases following the formation of plateletlike structures at 475 °C. Extended internal surfaces develop around 550 °C leading to the exfoliation of GaN thin layer. © 2008 American Institute of Physics.

[DOI: 10.1063/1.2955832]

GaN is attracting a great deal of attention as a promising semiconductor for environmentally compatible solid-state lighting and advanced optoelectronics. The emerging technologies still face major challenges due to the limited quality of the heteroepitaxial structures and to the high price of freestanding (fs) GaN wafers. The ion-cut process holds promise for overcoming these obstacles in an analogous scheme as for the mature technology of silicon on insulator.¹ In this process, implanted H and/or He ions act as an atomic scalpel which allows the transfer of bulk quality thin layers onto different host materials accomplishing a wide variety of heterostructures frequently unattainable by epitaxy. The ion-cut process has been applied to various semiconductor materials such as Ge, InP, and GaAs.² Independently of the material, the interaction of the implanted species with the radiation damage seems to play the key role in the splitting process. Apart from Si which was intensively investigated,³ only few studies were devoted to investigate the atomic processes involved in the splitting of other semiconductors.⁴ GaN exfoliation induced by H implantation was reported by Kucheyev *et al.*⁵ However, detailed studies on the mechanisms of ion slicing of GaN are still missing. Understanding these fundamental aspects is vital in order to control and optimize the ion-cut process. This letter sheds some light on structural details of H-implanted fs-GaN and critical transformations leading to thin layer exfoliation.

~300- μm -thick 2 in. double side polished undoped fs-GaN wafers were used in this study. The wafers were subject to room temperature H implantation at 50 keV with a fluence of 2.6×10^{17} atom/cm². A number of samples, as implanted or annealed at different temperatures, were analyzed using cross-sectional transmission electron microscopy (XTEM), high resolution x-ray diffraction, Rutherford backscattering in channeling mode (RBS/C), elastic recoil detection (ERD), and positron annihilation spectroscopy (PAS). The annealing time was ~1–2 min.

Several atomic processes take place during the implantation of energetic H ions generating defects from both sub-

lattices. H-defect interactions in GaN were already investigated for very low⁶ and high implantation doses under different annealing protocols.⁷ The experimental window for ion cutting is in between these two extreme cases. In Fig. 1, we summarize GaN postimplantation structural properties. The XTEM micrograph [Fig. 1(a)] shows a broad damage band extending over a 300-nm-thick layer starting about 200 nm below the surface. No extended defects are observed at the implanted fluence. High magnification images of the implanted zone taken under focus (not shown) indicate the presence of a high density of nanoscopic bright spots of ~1–2 nm diameter. The change in their contrast during focus variation suggests that they are voidlike structures.⁸ We name these nanoscopic voids nanobubbles. Figure 1(b) dis-

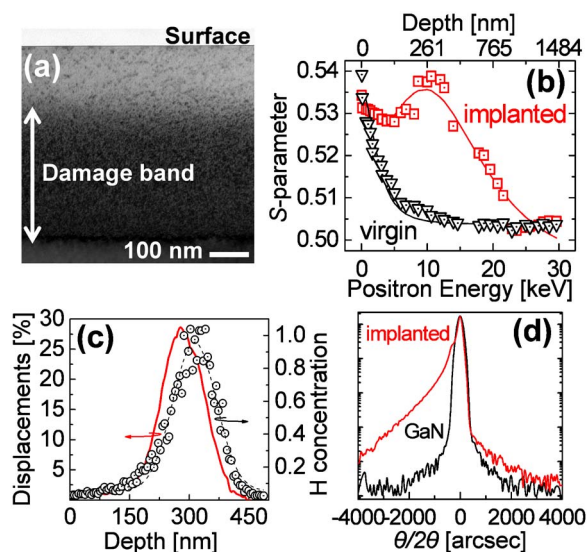


FIG. 1. (Color online) (a) XTEM image of damage induced in GaN by H ion implantation at 50 keV with a fluence of 2.6×10^{17} atom/cm². (b) *S* parameter depth profile measured before (triangles) and after (squares) H implantation. (c) H concentration/ 10^{22} cm⁻³ depth profile (circles) and implantation damage profile (line) as deduced from ERD and ion channeling, respectively. (d) X-ray $\theta/2\theta$ scans of (0002) GaN before and after H implantation.

^{a)}Electronic mail: moutanab@mpi-halle.mpg.de.

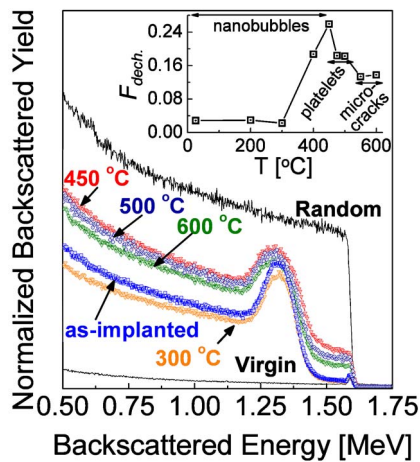


FIG. 2. (Color online) RBS/C yields as a function of annealing temperature for GaN substrates implanted with H at 2.6×10^{17} atom/cm². Inset: Evolution of dechanneling factor $F_{\text{dech.}}$ as a function of temperature. The corresponding morphologies, as determined by XTEM, are also indicated.

plays Doppler broadening S parameter depth profiles measured before and after implantation. In the implanted region an enhancement of the S parameter of 6.5% is observed [Fig. 1(b)], indicating the presence of open volume defects which support XTEM observations. Such an increase is too large to be caused by monovacancies; obviously small vacancy clusters are detected. Figure 1(c) displays H and atomic displacement depth profiles in as-implanted GaN as deduced from ERD and ion channeling analyses, respectively. The data show that H distribution is peaked at ~ 320 nm in agreement with SRIM calculations.⁹ H concentration at the peak is found to be $\sim 1.2 \times 10^{22}$ H/cm³ corresponding to an atomic concentration of about $\sim 13\%$ which is approximately three times higher than the concentration needed for Si exfoliation.³ The atomic displacement field reaches a maximum of $\sim 27\%$ at a shallower depth around 285 nm. We estimate the displacements per ion to be ~ 2.5 , much smaller than ~ 10 calculated at a lattice temperature of 0 K (i.e., without dynamic annealing).⁹ This suggests that about 75% of Frenkel pairs recombine during the implantation process. This annihilation rate is relatively smaller than in the case of Si implanted under ion-cut conditions.³ Therefore, the dynamic annealing cannot explain the unusually high fluence required for the splitting of GaN. The nature of H-defect complexes and their thermal evolution may play the most critical role than the absolute amount of the surviving defects. X-ray diffraction spectrum of H-implanted GaN evidences the presence of an out-of-plane tensile stress detected as a shoulder extending from the left side of the GaN (0002) peak [Fig. 1(d)]. Postimplantation wafer curvature measurement indicates that this out-of-plane tensile strain is accompanying an in-plane biaxial compressive stress estimated to be in the order of ~ 1.4 GPa. This built-in compressive stress has an undesirable impact on H-induced GaN layer transfer technology as it leads to a strong bowing of fs-GaN (Ref. 10) making the bonding of H-implanted wafers exceedingly difficult. Innovative approaches are needed to overcome this technological problem.

In Fig. 2, normalized RBS/C spectra from H-implanted GaN samples are displayed, either at RT, or after annealing at the indicated temperatures. The ratio between the virgin and random data is found to be much smaller than the case of GaN layers grown on sapphire.¹¹ This is due to the high

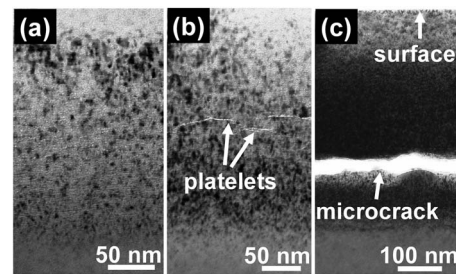


FIG. 3. XTEM micrographs of H-implanted GaN annealed at different temperatures: 450 °C (a), 500 °C (b), and 600 °C (c).

crystalline quality of fs-GaN substrates used in this study. With a density of dislocations in the order of 10^7 cm⁻², these substrates are more suitable to investigate impurity-defect interactions. H implantation creates a peak in the ion channeling yield centered at ~ 1.32 MeV. Its classic interpretation would be the direct scattering on displaced atoms in lattice channels. However, under ion-cut conditions, implantation-induced structures such as nanobubbles, point defect clusters, dislocations, and H-defect complexes can also induce a strong localized lattice deformation leading to an increase of the dechanneling yield [see Ref. 12 and references therein]. The particular influence of each defect or complex was elegantly treated by Feldman *et al.*¹³ It is important to note that no lattice disorder is observed near the surface.

RBS/C yield slightly decreases after heating at 300 °C. This can be attributed to the return of some interstitial atoms to substitutional sites. RBS/C spectra recorded after annealing at higher temperatures show unexpected features. The first is a strong broadening of damage-related peak observed only at the left side for backscattered energies below 1.28 MeV. The second feature in the spectra is the increase of dechanneling beyond the implanted zone. Finally, annealing above 300 °C causes also a strong enhancement of dechanneling near the surface. Note that the increase of the peak intensity comes simply from the increase of dechanneling *background*. Interestingly, the dechanneling level decreases above 450 °C.

Annealed samples were also analyzed using XTEM. In Fig. 3, we show a representative set of XTEM images. We note that annealing up to 450 °C does not trigger any significant morphological changes in the damage band [Fig. 3(a)]. Similarly to the as-implanted sample, the implanted zone remains decorated with nanobubbles. A small increase in temperature above 450 °C leads to the formation of nanoscopic cracks or platelets parallel to the surface [Fig. 3(b)]. Further increase in the annealing temperature induces large cracks leading to a complete exfoliation of a ~ 340 -nm-thick layer. Our detailed XTEM data show that structural transitions from nanobubbles to platelets and from platelets to microcracks occur within temperature windows as narrow as 25 and 50 °C, respectively. 450 °C is identified as the critical temperature at which transformation processes commence. Interestingly, at this temperature, the dechanneling enhancement in RBS/C yield attains its maximum (Fig. 2). To characterize the evolution of this enhancement, we introduce the factor $F_{\text{dech.}}$ which can be associated to lattice disorder:¹³ $F_{\text{dech.}}(E_{\text{BS}}) = \ln[(1 - \chi_v)/(1 - \chi_D)]$, where χ_D is the channeled backscattering yield divided by the random yield, and χ_v is the corresponding quantity for the virgin substrate at the same backscattered energy E_{BS} . The inset of Fig. 2

displays the evolution of $F_{\text{dech.}}$ as a function of annealing temperature. The calculations were performed at $E_{\text{BS}} = 1.52$ MeV near the surface. The corresponding morphologies are also indicated. We note that $F_{\text{dech.}}$ saturates at 450 °C and monotonically decreases above this temperature. It is noteworthy that $F_{\text{dech.}}$ calculated for backscattered energies at the damage peak and beyond the implanted region are found to behave qualitatively similar to the data reported in Fig. 2 (inset). This suggests that the same kind of defects or complexes gives rise to all features observed in postannealing RBS/C spectra (Fig. 2). Since thermal annealing cannot create self-interstitials, dechanneling enhancement indicates that other structural defects are involved. This enhancement is different from what was observed in H-induced Si blistering where the relative increase in backscattering yield was found to be much more pronounced near the surface than beyond the damage layer.^{12,14} This *irreversible* effect was attributed to the macroscopic deformation of blisters cap.¹⁴ Our atomic force microscopy analysis shows that GaN surface remains unchanged up to 550 °C in agreement with detailed blistering kinetics study reported earlier.¹⁵ It is also worth to mention that the macroscopic swelling and surface elevation of ion implanted GaN is always accompanied by the formation of very large cavities.¹⁶ Remember, however, that annealing up to 450 °C does not induce any significant change in nanobubbles size [Fig. 3(a)]. Also, the decrease in $F_{\text{dech.}}$ above 450 °C indicates that the phenomenon behind dechanneling enhancement is *reversible* in contrast to the case of surface deformation.¹⁴ This drives us to suggest that strain-induced lattice distortions could be at the origin of this unexpected thermoevolution of RBS/C spectra during nanobubbles *regime*. A possible origin of lattice distortion would be H₂ molecules trapping in nanobubbles leading to the buildup of internal pressure. However, highly pressurized nanobubbles *alone* cannot explain the observed dechanneling since their stress field can hardly reach the surface. Since damage layer contain also other defect complexes such as self-interstitial clusters, one can suppose that their combined influence with hydrogen-induced internal pressure can increase the in-plane compressive strain causing a strong lattice distortion. This process will ultimately lead to a weakening of the atomic bonding. The system attains the criticality around 450 °C. $F_{\text{dech.}}$ decreases above this temperature suggestive of a partial relief of the internal strain following the formation of platelets parallel to the surface. These platelets define the fracture paths for the exfoliation. Interestingly, Doppler broadening measurements for samples annealed at $T \leq 450$ °C were found to be identical to as-implanted state [Fig. 1(b)]. The absence of vacancy clustering in this temperature range indicates that the necessary void for splitting assembles dynamically during the implantation process. This behavior differs completely from the evolution observed in Si where an important increase of voidlike defects was found to proceed the exfoliation.¹² In a recent model,¹⁷ damage-induced in-plane compressive strain was suggested as the driving force for vacancy agglomeration leading to platelets formation in Si. The same description was also used to explain H-induced InP exfoliation.¹⁸ However, the remarkable difference in vacancylike defects thermal behavior observed between GaN and Si suggests that a general and predictive microscopic model of ion-cut process has to consider the intrinsic properties of the material, the nature of H-defect complexes, and point defects diffusiv-

ity. These aspects are still poorly understood for GaN. Additional systematic experimental studies and calculations would be highly valuable. Finally, despite that H₂ is believed to play a crucial role, probing and understanding its exact thermal behavior in GaN under ion-cut conditions will remain an open challenge as it is still for Si.³ The only available data from first-principles calculations demonstrate that H₂ in GaN requires unfavorably high formation energy (~ 2.4 eV in vacuum) compared to Si.¹⁹ This could explain in part the high fluence needed for GaN ion cutting.

In summary, we investigated the critical structural transformations involved in splitting of GaN by H implantation and subsequent annealing. We found that vacancy clustering during the implantation process leads to assembly of 1–2 nm nanobubbles. Temperatures of 300–450 °C give rise to a strong enhancement of dechanneling tentatively attributed to strain-induced lattice distortion. At higher temperature, the dechanneling is partially reduced following the formation of platelets indicative of a partial relief of the strain. These platelets define the fracture path for the exfoliation. Extended internal surfaces develop around 550 °C leading to splitting of ~ 340 -nm-thick layer. Our result is a first step toward understanding the basic mechanisms of GaN ion cutting.

The CrysGaN project funded by the German Federal Ministry of Education and Research (BMBF) partially contributed to this work.

¹M. Bruel, *Electron. Lett.* **31**, 1201 (1995).

²Q.-Y. Tong, Y.-L. Chao, L.-J. Huang, and U. Gösele, *Electron. Lett.* **35**, 341 (1999); L. Di Cioccio, E. Jalaguier, and F. Letertere, *Phys. Status Solidi A* **202**, 509 (2005).

³For a recent review, see, B. Terreault, *Phys. Status Solidi A* **204**, 2129 (2007).

⁴A. Fontcuberta, I. Morral, J. M. Zahler, M. J. Griggs, H. A. Atwater, and Y. J. Chabal, *Phys. Rev. B* **72**, 085219 (2005); J. M. Zahler, A. Fontcuberta, I. Morral, M. J. Griggs, H. A. Atwater, and Y. J. Chabal, *Phys. Rev. B* **75**, 035309 (2007).

⁵S. O. Kucheyev, J. S. Williams, C. Jagadish, J. Zou, and G. Li, *J. Appl. Phys.* **91**, 3928 (2001).

⁶M. G. Weinstein, C. Y. Song, M. Stavola, S. J. Pearton, R. G. Wilson, R. J. Shul, K. P. Killeen, and M. J. Ludowise, *Appl. Phys. Lett.* **72**, 1703 (1998).

⁷C. H. Seager, S. M. Myers, G. A. Peterson, J. Han, and T. Headley, *J. Appl. Phys.* **85**, 2568 (1999).

⁸I. Radu, R. Singh, R. Scholz, U. Gösele, S. Christiansen, G. Brüderl, C. Eichler, and V. Härle, *Appl. Phys. Lett.* **89**, 031912 (2006).

⁹J. F. Ziegler, J. B. Biersack, and U. Littmark, *The Stopping and Range of Ions in Solids* (Pergamon, New York, 1985).

¹⁰R. Singh, I. Radu, G. Brüderl, C. Eichler, V. Haerle, U. Gösele, and S. H. Christiansen, *Semicond. Sci. Technol.* **22**, 418 (2007).

¹¹W. R. Wampler and S. M. Myers, *MRS Internet J. Nitride Semicond. Res.* **4S1**, G3.73 (1999).

¹²O. Moutanabbir, B. Terreault, M. Chicoine, F. Schiettekatte, and P. J. Simpson, *Phys. Rev. B* **75**, 075201 (2007).

¹³L. C. Feldman, J. W. Mayer, and S. T. Picraux, *Materials Analysis by Ion Channeling* (Academic, New York, 1982).

¹⁴R. Tonini, F. Corni, C. Nobili, G. Ottaviani, F. Cazzaniga, and G. Queirolo, *Solid State Phenom.* **82**, 291 (2002).

¹⁵R. Singh, I. Radu, U. Gösele, and S. H. Christiansen, *Phys. Status Solidi C* **3**, 1754 (2006).

¹⁶S. O. Kucheyev, J. S. Williams, C. Jagadish, J. Zou, V. S. J. Craig, and G. Li, *Appl. Phys. Lett.* **77**, 1455 (2000).

¹⁷M. Nastasi, T. Höchbauer, J.-K. Lee, A. Misra, J. P. Hirth, M. Ridgway, and T. Lafford, *Appl. Phys. Lett.* **86**, 154102 (2005).

¹⁸P. Chen, Z. Di, M. Nastasi, E. Bruno, M. G. Grimaldi, N. D. Theodore, and S. S. Lau, *Appl. Phys. Lett.* **92**, 202107 (2008).

¹⁹J. Neugebauer and C. G. Van de Walle, *Phys. Rev. Lett.* **75**, 4452 (1995).